AIP Journal of Applied Physics

Low voltage tunneling magnetoresistance in CuCrO2-based semiconductor heterojunctions at room temperature

X. R. Li, M. J. Han, J. D. Wu, C. Shan, Z. G. Hu, Z. Q. Zhu, and J. H. Chu

Citation: Journal of Applied Physics **116**, 223701 (2014); doi: 10.1063/1.4903733
View online: http://dx.doi.org/10.1063/1.4903733
View Table of Contents: http://scitation.aip.org/content/aip/journal/jap/116/22?ver=pdfcov
Published by the AIP Publishing

Low voltage tunneling magnetoresistance in $CuCrO_2$-based semiconductor heterojunctions at room temperature

X. R. Li (李旭瑞),[1] M. J. Han (韩美杰),[1] J. D. Wu (吴嘉达),[2] C. Shan (单超),[1]
Z. G. Hu (胡志高),[1,a)] Z. Q. Zhu (朱自强),[1] and J. H. Chu (褚君浩)[1]
[1]*Key Laboratory of Polar Materials and Devices, Ministry of Education, Department of Electronic Engineering, East China Normal University, Shanghai 200241, China*
[2]*Department of Optical Science and Engineering, Fudan University, Shanghai 200433, China*

(Received 23 July 2014; accepted 25 November 2014; published online 8 December 2014)

$CuCrO_2$-based heterojunction diodes with rectifying characteristics have been fabricated by combining *p*-type Mg-doped $CuCrO_2$ and *n*-type Al-doped ZnO. It was found that the current for the heterojunction in low bias voltage region is dominated by the trap-assisted tunneling mechanism. Positive magnetoresistance (MR) effect for the heterojunction can be observed at room temperature due to the tunneling-induced antiparallel spin polarization near the heterostructure interface. The MR effect becomes enhanced with the magnetic field, and shows the maximum at a bias voltage around 0.5 V. The phenomena indicate that the $CuCrO_2$-based heterojunction is a promising candidate for low-power semiconductor spintronic devices. © *2014 AIP Publishing LLC*.
[http://dx.doi.org/10.1063/1.4903733]

I. INTRODUCTION

Spin-based device is an emerging technology, which leads to the potential for new classes of ultra-low power, high speed memory, logic and photonic devices. Unlike traditional semiconductor devices in integrated circuits, spin-based devices perform their specific functions such as signal-processing or information-storage by controlling the spin injection and transport rather than the charge of the carriers.[1] For example, mass storage of modern information technology based on magnetic recording takes advantage of the spin of electrons in metals or semiconductors. Metal-based spintronic devices based on the principle of magnetoresistance (MR) effect have already been commercially used in several technologies such as hard disk drives and magnetoresistive random-access memory (MRAM).[2] Semiconductor-based spintronics offers a possible direction towards the development of devices that could perform logic, communications, and storage functions within a single material system.[3] Unfortunately, most semiconductor spintronic devices can only work at low temperatures, which limit their potential applications.

Recently, delafossite structured $CuCrO_2$ has attracted much more attention as a promising *p*-type transparent conducting oxide (TCO) semiconductor. Hole-doped $CuCrO_2$ is a wide band material with low resistivity. Upon doping with 5% Mg, the $CuCrO_2$:Mg film shows the lowest resistivity of 0.0045 Ω cm among *p*-type TCOs.[4] Spin characteristic is another attractive point for the triangular lattice antiferromagnet (TLA) $CuCrO_2$. The spin- and electric-state of Cr^{3+} ions make a large contribution to the electrical and magnetic behaviors of $CuCrO_2$ system.[5] Furthermore, room-temperature ferromagnetism for the delafossite-structured ABO_2 TCOs like $CuCrO_2$ and $CuAlO_2$ has already attracted much attention. Impurity doped $CuCrO_2$ can even possess a Curie temperature much above room temperature (RT), which indicates the potential application of spin characteristics at RT.[6–8] On the other hand, as a traditional *n*-type TCO with wide band gap and controllable electrical resistivity, impurity-doped ZnO has been selected to fabricate *p-n* heterojunctions combining *p*-type $CuCrO_2$. $CuCrO_2$ has a structure symmetry compatible with sapphire and ZnO. The $CuCrO_2$/ZnO heterojunction diodes fabricated by pulsed laser deposition (PLD) have been proved to possess high optical transparency and rectifying characteristic.[9] Nevertheless, the spin characteristics for $CuCrO_2$/ZnO *p-n* heterojunctions have not been studied. By investigating the spin characteristics for $CuCrO_2$-based TCO junctions, a possible mechanism for read-out in semiconductor spintronics is explored.

In this article, *p*-type Mg-doped $CuCrO_2$ ($CuCrO_2$:Mg) and *n*-type Al-doped ZnO (ZnO:Al) are selected to fabricate *p-n* heterojunctions. Transport mechanisms of the heterojunctions in different bias voltage regions have been studied from current-voltage (*I-V*) characteristics at different temperatures. The spin and electrical properties for the heterojunction diodes have been investigated under different magnetic fields. It has been manifested that the antiparallel spin polarization induced by the trap-assisted tunneling effect results in the positive MR of heterojunction diode.

II. EXPERIMENTAL DETAILS

The structure of *p*–($CuCrO_2$:Mg)/*n*–(ZnO:Al) heterojunction diodes is shown in Fig. 1(a). First, nanocrystalline $CuCrO_2$:Mg films were prepared on (001) sapphire substrates by the sol-gel route employing a spin-coating process. A detailed fabrication procedure can be found in Ref. 10. Heterojunction was formed by depositing a 100 nm thick *n*-type Al doped ZnO (with 5% Al concentrations) film by the PLD technique in an O-rich ambient with an appropriate mask on the surface.[11] The film undergoes a post-thermal

a)Author to whom correspondence should be addressed. Tel.: +86-21-54345150. Fax: +86-21-54345119. Electronic mail: zghu@ee.ecnu.edu.cn

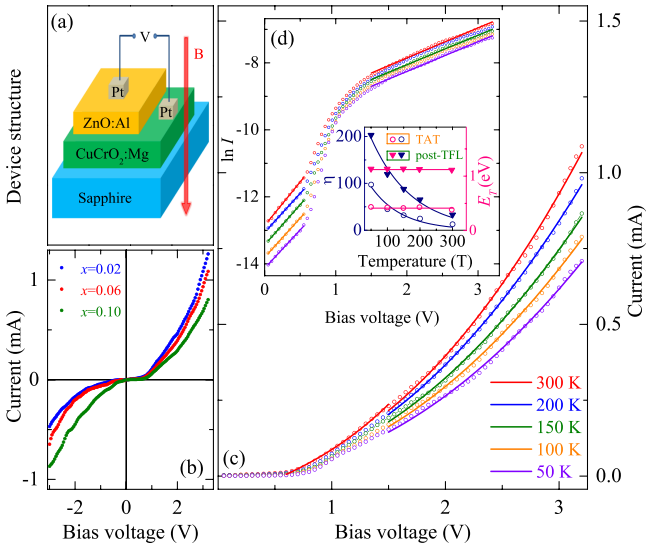

FIG. 1. (a) Device structure for $CuCrO_2$:Mg/ZnO:Al heterojunctions. (b) *I-V* characteristics of the $CuCr_{1-x}Mg_xO_2$/ZnO:Al ($x = 0.02, 0.06, 0.10$) heterojunctions measured in the absence of magnetic field at RT. (c) *I-V* characteristics at different temperatures for the $CuCr_{0.94}Mg_{0.06}O_2$/ZnO:Al heterojunction. (d) The plot of ln*I vs. V* at different temperatures for the $CuCr_{0.94}Mg_{0.06}O_2$/ZnO:Al heterojunction. The empty circles and the solid triangles in the inset represent temperature-dependent ideality factor η and energy barriers E_T for $CuCr_{0.94}Mg_{0.06}O_2$/ZnO:Al heterojunction in TAT region and post-TFL region, respectively.

annealing at 500 °C for 30 min. The contacts were completed by depositing platinum (Pt) on both $CuCrO_2$:Mg and ZnO:Al layers through an appropriate mask in vacuum. All contacts obey the Ohmic behavior, which can be verified by the linear *I-V* property (not shown). The single-layer $CuCrO_2$:Mg films have been proved to possess good conductivity and high transmittance. The Curie temperature for the $CuCrO_2$:Mg film stays around RT according to the results from Raman spectra.[4,10] The carrier concentration at RT for ZnO:Al film here is on the magnitude of about 4×10^{21} cm^{-3}. *I-V* characteristics and Van der Pauw measurements were done on a home-build system, which is based on an Oxford Spectromag SM4000 magnetic system equipped with a series of precise electrical instruments: the current source (Keithley 6221), the digital nanovoltmeter (Keithley 2182 A), the switch mainframe (Keithley 7001) with a Hall-effect card (Keithley 7065) inside. In addition, the sub-femtoamp remote sourcemeter (Keithley 6430) is used as a supplement for high-resistance measurements.[4]

III. RESULTS AND DISCUSSION

Typical *I-V* characteristics of the $CuCr_{1-x}Mg_xO_2$/ZnO:Al ($x = 0.02, 0.06, 0.10$) heterojunctions have been measured in the absence of magnetic field. The bias voltage was tuned with a step of 0.05 V. As can be seen in Fig. 1(b), rectifying behavior can be observed, which manifests the quality of the heterojunctions. The ideality factor η of a diode can be determined from the slope of a linear part for the forward bias ln*I vs. V* curve according to the equation: $\eta = (q/kT)[dV/d(\ln I)]$, where q is the elementary charge and k is the Boltzmann constant.[12] The η is much larger than 2 in the whole bias region. This phenomenon has also been observed in some other wide band gap *p-n* junctions, indicating that there are additional transport mechanisms other than diffusion and recombination.[13]

To determine the transport mechanisms for the heterojunctions, *I-V* characteristics have been studied at different temperatures. For example, the plots of ln*I vs. V* at different temperatures for $x = 0.06$ are plotted in Fig. 1(c). It is obvious that the slope for ln*I vs. V* ($S_{\ln}$) shows a bias-dependent trend. At low bias voltages, the $S_{\ln}$ is kept the same at all temperatures. By denoting the characteristic barrier energy $E_T = q/S_{\ln} = \eta kT$, the E_T at low bias region is insensitive to temperature, as shown in the inset of Fig. 1(d), indicating that the transport through the interface is dominated by the tunneling mechanism. It is because the voltage variation of the tunneling current is dominated by the tunneling probability, which is not distinctly affected by temperature.[14] The tunneling current in low bias region is primarily the trap-assisted tunneling (TAT) current through the trap defect energy levels.[14,15] The inset of Fig. 1(d) also shows the calculated η at different temperatures in each bias voltage region. The decreasing ideality factor with increasing temperature indicates less leakage current from tunneling. The activation of acceptors and donors is elevated with increasing temperature, attenuating the influence from trap defects on the transport properties. Therefore, the TAT current is suppressed at higher temperatures. As the bias voltage increases above 0.5 V, the $S_{\ln}$ becomes temperature-dependent, suggesting that another transport mechanism becomes dominant over conduction via tunneling. In this bias voltage region, a space charge field can be created by increasing injected carriers into the device. The current is dominated by this field, which is known as the space charge limited (SCL) current.[16] As shown in Fig. 1(c), the *I-V* curve shows a $I \propto V^n$ ($n > 2$) trend, indicating that the current is dominated by the trap-controlled SCL mechanism.[17] The current is suppressed in the presence of traps because the free carrier charges can be captured by the trap centers. The $S_{\ln}$ is temperature dependent in this region because E_T is dependent on the trap density, which is affected by the temperature.[18] As the voltage increases, the increasing injected charge carrier density also results in the filling of a larger number of traps. After reaching a voltage at which all the traps are filled, the temperature variation of $S_{\ln}$ gradually fades away due to temperature-independent E_T. The *I-V* curves in this region can be expressed as the post trap filled limit (post-TFL) pattern, where the *I-V* curves are independent of the trap distribution in the energy space. The approximate Mott's V^2 law ($I \propto V^2$) at high voltages can support this model well. The appearance of post-TFL pattern indicates that the traps are distributed discretely at a single level other than exponentially in the energy space.[18]

Device resistance (R_D) at different bias voltages for $CuCr_{0.94}Mg_{0.06}O_2$/ZnO:Al heterojunction under magnetic field of 0 and 5 T and the temperature of 300 and 150 K is shown in the inset of Fig. 2. Here, R_D is obtained from the *I-V* curve and can be expressed as V/I. R_D shows a bias-dependent trend due to the combined action of different transport mechanisms. The discrepancy of R_D at different magnetic fields indicates the appearance of MR effect. Here,

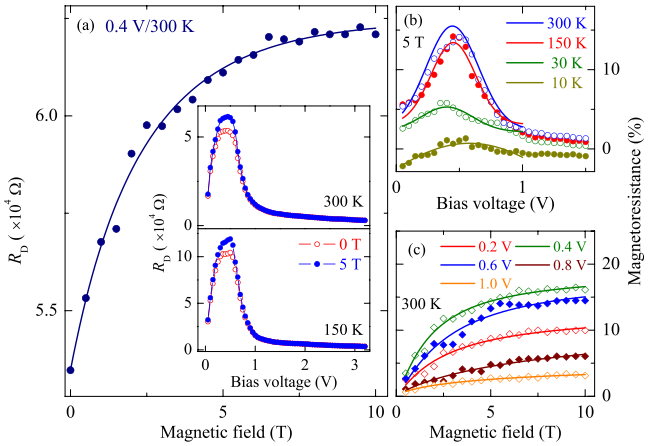

FIG. 2. (a) The evolution of room-temperature R_D with magnetic field for the heterojunction device at a typical bias voltage 0.4 V. Bias-voltage dependent device resistance R_D under the magnetic field of 0 and 5 T for $CuCr_{0.94}Mg_{0.06}O_2$/ZnO:Al heterojunction at 300 K and 150 K is shown in the inset of (a). (b) The bias-voltage dependent MR of the heterojunction device at different temperatures under a magnetic field of 5 T. (c) The evolution of room-temperature MR with magnetic field for the heterojunction device at different bias voltages. Note that the solid lines are applied to guide the eyes.

the value of MR is defined as $(R_B - R_0)/R_0 \times 100\%$, where R_B denotes the resistance under a magnetic field B and R_0 represents the resistance outside a magnetic field. Fig. 2(a) shows that R_D increases with magnetic field at a certain bias voltage, which manifests the MR effect directly. It can be observed from Fig. 2(b) that the device shows obviously positive MR effect below 1 V, and exhibits the strongest MR effect at the bias voltage around 0.5 V. The value of MR for the heterojunction increases with the magnetic field and gradually approaches a constant, as can be seen from Fig. 2(c). To study the origin of the MR effect in detail, the resistance of single-layer $CuCr_{0.94}Mg_{0.06}O_2$ and ZnO:Al individual films at different magnetic fields is studied, respectively. Negative MR can be clearly observed from the $CuCr_{0.94}Mg_{0.06}O_2$ film in low temperature region, as shown in Fig. 3. Magnetic properties of $CuCrO_2$:Mg are dominated by the triangular lattice planes formed by Cr^{3+}ions.[5] It has

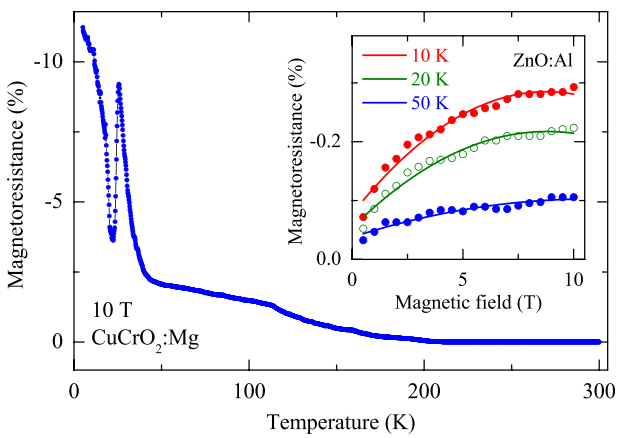

FIG. 3. Negative MR effect for single-layer $CuCr_{0.94}Mg_{0.06}O_2$ film at different temperatures under a magnetic field of 10 T. The inset shows the value of MR for single-layer ZnO:Al film at extremely low temperatures. Note that the solid lines are applied to guide the eyes.

been manifested that there is a transition of carrier transport mechanism from a thermal activation behavior to a variable range hopping (VRH) one at a special temperature T_{cross}.[19] In the temperature region below T_{cross}, the decrease of the thermal energy depresses the hopping between the nearest-neighbor Cu sites. The contributions from the hopping to the Cr sites and Cu sites in the other layers (but with closer energy) become relatively dominant. The correlation between the hole and the local spin at the Cr site becomes stronger. External magnetic field reduces the fluctuation of the local spins and makes the localization around Cr sites stronger. The enhanced localization reduces the carrier scattering and results in a clear negative MR in the VRH region.[20] Moreover, negative MR effect becomes stronger and shows a sharp oscillation with temperature at extremely low temperatures. It has been suggested that the $CuCrO_2$:Mg undergoes two successive magnetic phase transitions in low temperature region at corresponding Néel temperatures.[5] The enhancement of negative MR is a typical behavior of the spin-charge coupling near the magnetic phase transitions.[19] The oscillation of the negative MR is ascribed to the influence on spin fluctuations from localized magnetic moments during the collinear antiferromagnetic phase.[21] The inset of Fig. 3 shows that the nonmagnetic material ZnO:Al also has a negative MR at extremely low temperatures. It can be well described by a semiempirical expression that takes into account the third order *s-d* exchange Hamiltonians, which describes a negative part and a two-band model for positive contribution.[22] Nevertheless, the value is quite small, as compared to that of $CuCrO_2$:Mg and the heterojunction structure.

The MR effect of the individual films is negative at low temperatures and gradually approaches zero, indicating that the positive MR effect for the junction is associated with the interface effect. As we know, tunnel MR (TMR), anisotropic MR (AMR), and tunnel anisotropic MR (TAMR) are traditional interfacial MR effects. In contrast to TMR (which is a consequence of spin-dependent tunneling), AMR originates from spin-orbit coupling, which is present in all magnetic materials.[23] And TAMR is only an anisotropic dependence with the direction of magnetization based on TMR, which is usually very small (only a few percent of TMR).[24] Both AMR and TAMR depend on the angle between the current direction and the local magnetization. However, the MR effect here shows no obvious dependence on the angular of the applied field direction, indicating that the heterojunctions are free of anisotropic influence to a certain degree. In addition, atomic force microscope (AFM) and scanning electron microscope (SEM) measurements manifest that MgO layer has not been obviously formed. The results of X-ray diffraction (XRD) and Raman measurements prove that there exists little spinel phase of $MgCr_2O_4$ or MgO for the $CuCr_{0.94}Mg_{0.06}O_2$/ZnO:Al structure. It indicates that the spin-filtering from MgO can be ignored when electrons tunnel.[10] To explore the primary origin of the positive MR effect for the heterojunction in detail, an electronic band structure diagram for the heterojunction device has been presented in Fig. 4. It suggests that the Fermi energy lies above the conduction band minimum for ZnO doped with 5% Al.[22]

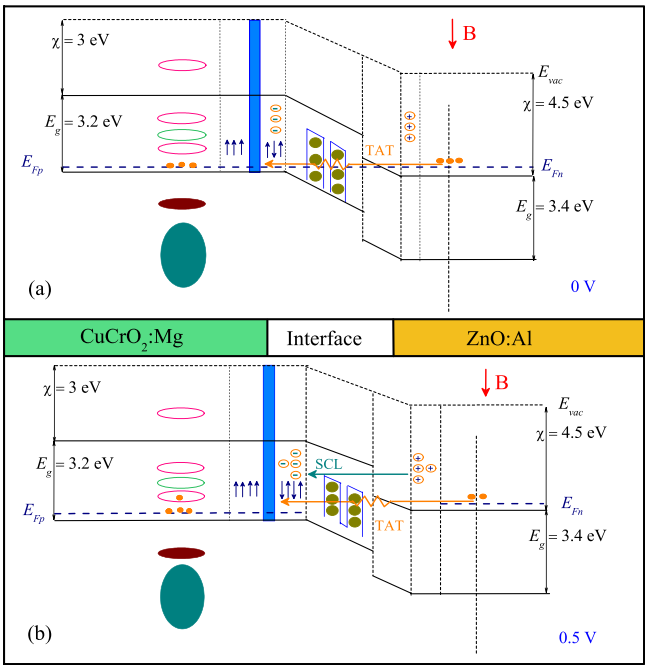

FIG. 4. Electronic band structure diagrams for the heterojunction at a bias voltage of (a) 0 V and (b) 0.5 V are applied to explain the origin of positive MR effect.

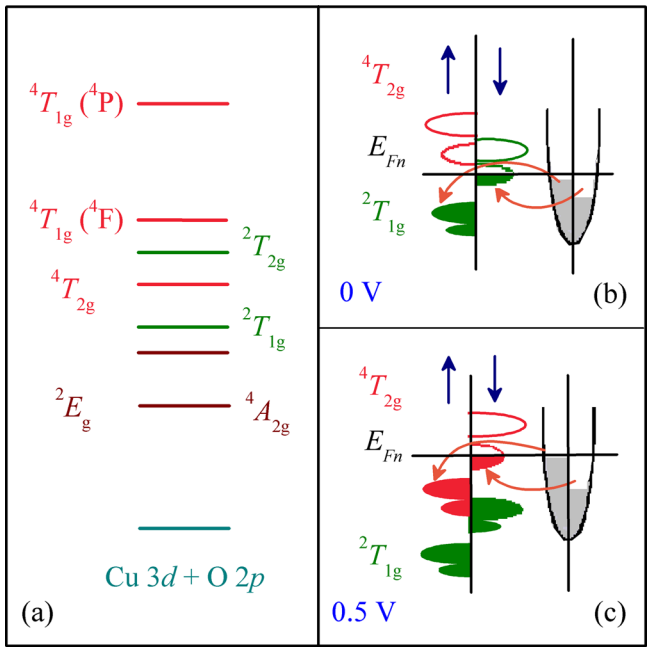

FIG. 5. (a) Schematic band diagram for the $CuCr_{0.94}Mg_{0.06}O_2$ film under an octahedral crystal field. (b) The spin polarization of the spin-down and spin-up carriers on each side of the tunneling-induced barrier. Carriers from ZnO:Al tunneling into different sub-bands of $CuCr_{0.94}Mg_{0.06}O_2$ at a bias voltage of 0 V and 0.5 V are shown in (c) and (d), respectively.

Here, the relatively small spin and splitting effect for the nonmagnetic ZnO:Al can be neglected. The electron affinity (χ) and the band gap energy (E_g) for ZnO:Al here are taken as 4.5 eV and 3.4 eV, while for $CuCrO_2$:Mg they are 3 eV and 3.2 eV, respectively.[12,25] It has recently been reported that the near-Fermi-level (around the valence band maximum) of $CuCrO_2$:Mg has primarily the Cr 3*d* characteristics, with some contributions from the hybridization of Cu 3*d* and O 2*p* states.[26,27] The octahedral crystal field leads to the splitting of the Cr 3*d* orbital energies, as shown in Fig. 5(a). The d_{xy}, d_{xz}, and d_{yz} orbitals at lower energy are collectively called as the t_{2g} orbitals, whereas the d_{z^2} and $d_{x^2-y^2}$ orbitals at higher energy are called as the e_g orbitals. The $3d^3$ states of Cr^{3+} ion in an octahedral environment originally have a ${}^3t_{2g}$ configuration with a ground state ${}^4A_{2g}$ and an excited state ${}^2E_g$. Meanwhile, the ligands that surround the Cr^{3+} ion introduce additional negative charges and make the *d* orbitals less stable. Then, the Cr 3*d* splitting energy possesses three electron configuration combinations arranged in elevating energy: ${}^3t_{2g}$, ${}^2t_{2g}{}^1e_g$, and ${}^1t_{2g}{}^2e_g$. The ${}^2t_{2g}{}^1e_g$ configuration gives rise to two low lying quartet states [${}^4T_{2g}$ and ${}^4T_{1g}({}^4F)$ states], and the ${}^1t_{2g}{}^2e_g$ configuration induces a high lying quartet state [${}^4T_{1g}({}^4P)$].[28] Notice that all these Cr 3*d* states originally have the spin-up property.

When the magnetic field is applied, the degeneracy of the Cr 3*d* levels is further lifted by the operation of spin-orbit interaction according to Hund's rule. The degeneracy of a state is also considerably removed due to the Zeeman splitting in a magnetic state.[29] Focusing on the band gap around the Fermi-level of $CuCrO_2$:Mg (E_{Fp}), the ${}^2T_{1g}$ and ${}^4T_{2g}$ bands are further separated by Jahn-Teller distortion into two sub-bands, respectively.[30] Once the ZnO:Al is connected with $CuCrO_2$:Mg, electrons from *n*-type ZnO:Al can tunnel into the adjacent *p*-type $CuCrO_2$:Mg through the interfacial defects. It even partially fills the spin-down Cr ${}^2T_{1g}$ (${}^2T_{1g}\downarrow$) orbital after filling up the spin-up ${}^2T_{1g}$ (${}^2T_{1g}\uparrow$) state near the interface, as shown in Fig. 5(c). The density of carriers near the interface increases and an additional space-charge region is created. Then, a Schottky barrier will be built up to stop the further leaking of electrons into the homogeneous region of $CuCrO_2$:Mg.[31] In low bias region, the electrons can hardly pass through the barrier. Thus, the density of spin-down (minority-spin) carriers near the interface is much larger than that away from the interface. With increasing magnetic field, the spin polarization of the spin-down carriers near the interface and the spin-up (majority-spin) carriers is away from the interface both increase. The increasing scattering between carriers with antiparallel spin polarization results in the larger resistance under a magnetic field, as can be seen from Fig. 5(b).[32] Namely, the existence of minority-spin carriers in the hole-doped $CuCrO_2$:Mg near the interface under a magnetic field is the origin of the positive MR effect. With the magnetic field increases above 5 T, the spin polarization and Zeeman splitting effect gradually become saturated, making the MR of the heterojunction close to a constant. As shown in Fig. 4(b), the increasing forward bias voltage elevates the Fermi energy of ZnO:Al (E_{Fn}), as compared to E_{Fp}. The carriers can even partially fill the ${}^4T_{2g}\downarrow$ orbital after filling up the ${}^2T_{1g}\downarrow$ and ${}^4T_{2g}\uparrow$ states near the interface, as shown in Fig. 5(d). The increasing minority-spin carriers in the hole-doped $CuCrO_2$:Mg near the interface result in the enhancement of MR. When the bias voltage increases above 0.5 V, the electrons become easier to pass through the barrier. The density of minority-spin carriers in the homogeneous region is nearly the same as that in the interface region of $CuCrO_2$:Mg. Moreover, the current becomes dominated by the SCL transport mechanism. The

influence from the tunneling mechanism becomes weaker than that from the space charge field across the interface, which attenuates the MR effect. In addition, the MR effect at extremely low temperatures [such as 10 K and 30 K shown in Fig. 2(b)] is weaker than that at high temperatures. It is because the strong negative MR of the single-layer $CuCrO_2$:Mg impacts the positive MR effect from the interface tunneling.

IV. CONCLUSIONS

In summary, $CuCrO_2$:Mg/ZnO:Al heterojunctions have been fabricated with rectifying behaviors. The current of the diode at low bias voltage is dominated by the tunneling mechanism. The degeneracy of the Cr 3*d* states is lifted by the operation of spin-orbit interaction and Zeeman splitting when magnetic field is applied. Electrons from *n*-type ZnO:Al tunnel into the *p*-type $CuCrO_2$:Mg and even partially fill the spin-down orbitals in a magnetic state. The tunneling-induced barrier near the interface impedes the further leaking of carriers and makes the spin-down carriers only stay around the interface. The increasing scattering between the spin-down carriers near the interface and the spin-up carriers in the homogeneous region of $CuCrO_2$:Mg with antiparallel spin polarization results in the larger resistance under a magnetic field. In another word, the increasing spin polarization scattering induced by the spin tunneling effect under a magnetic field should be the primary origin of the positive MR effect for the diode according to the possible explanation proposed above. It can be anticipated that the favorable spin characteristics for the $CuCrO_2$-based devices will promote the RT application for semiconductor spintronics.

ACKNOWLEDGMENTS

This work was financially supported by Major State Basic Research Development Program of China (Grant Nos. 2011CB922200 and 2013CB922300), Natural and Science Foundation of China (Grant Nos. 11374097 and 61376129), Projects of Science and Technology Commission of Shanghai Municipality (Grant Nos. 14XD1401500, 13JC1402100, and 13JC1404200), and the Program for Professor of Special Appointment (Eastern Scholar) at Shanghai Institutions of Higher Learning.

[1]S. J. Peartona, C. R. Abernathy, D. P. Norton, A. F. Hebard, Y. D. Park, L. A. Boatner, and J. D. Budai, Mater. Sci. Eng. R **40**, 137 (2003).
[2]H. Ohno, Science **281**, 951 (1998).
[3]D. D. Awschalom and M. E. Flatté, Nat. Phys. **3**, 153 (2007).
[4]X. R. Li, M. J. Han, P. Chang, Z. G. Hu, Y. W. Li, Z. Q. Zhu, and J. H. Chu, Appl. Phys. Lett. **104**, 012103 (2014).
[5]K. Kimura, H. Nakamura, S. Kimura, M. Hagiwara, and T. Kimura, Phys. Rev. Lett. **103**, 107201 (2009).
[6]M. Jamet, A. Barski, T. Devillers, V. Poydenot, R. Dujardin, P. B. Guillemaud, J. Rothman, E. B. Amalric, A. Marty, J. Cibert, R. Mattana, and S. Tatarenko, Nat. Mater. **5**, 653 (2006).
[7]F. Lin, C. Gao, X. S. Zhou, W. Z. Shi, and A. Y. Liu, J. Alloys Compd. **581**, 502 (2013).
[8]C. J. Dong, W. X. Yu, M. Xu, J. J. Cao, Y. Zhang, Y. H. Chuai, and Y. D. Wang, J. Alloys Compd. **512**, 195 (2012).
[9]T. W. Chiu, K. Tonooka, and N. Kikuchi, Thin Solid Films **516**, 5941 (2008).
[10]M. J. Han, Z. H. Duan, J. Z. Zhang, S. Zhang, Y. W. Li, Z. G. Hu, and J. H. Chu, J. Appl. Phys. **114**, 163526 (2013).
[11]W. W. Li, Z. G. Hu, J. D. Wu, J. Sun, M. Zhu, Z. Q. Zhu, and J. H. Chu, J. Phys. Chem. C **113**, 18347 (2009).
[12]Y. G. Cao, L. Miao, S. Tanemura, M. Tanemura, Y. Kuno, and Y. Hayash, Appl. Phys. Lett. **88**, 251116 (2006).
[13]Y. W. Heo, Y. W. Kwon, Y. Li, S. J. Pearton, and D. P. Norton, Appl. Phys. Lett. **84**, 3474 (2004).
[14]X. A. Cao, E. B. Stokes, P. M. Sandvik, S. F. LeBoeuf, J. Kretchmer, and D. Walker, IEEE Electron Device Lett. **23**, 535 (2002).
[15]S. M. Yu, X. M. Guan, and H. S. P. Wong, Appl. Phys. Lett. **99**, 063507 (2011).
[16]D. S. Shang, Q. Wang, L. D. Chen, R. Dong, X. M. Li, and W. Q. Zhang, Phys. Rev. B **73**, 245427 (2006).
[17]T. H. Kim, K. S. Cho, E. K. Lee, S. J. Lee, J. Chae, J. W. Kim, D. H. Kim, J. Y. Kwon, G. Amaratunga, S. Y. Lee, B. L. Choi, Y. Kuk, J. M. Kim, and K. Kim, Nature Photon. **5**, 176 (2011).
[18]A. Jain, P. Kumar, S. C. Jain, V. Kumar, and R. M. Mehra, J. Appl. Phys. **102**, 094505 (2007).
[19]T. Okuda, N. Jufuku, S. Hidaka, and N. Terada, Phys. Rev. B **72**, 144403 (2005).
[20]J. Du, D. Li, Y. B. Li, N. K. Sun, J. Li, and Z. D. Zhang, Phys. Rev. B **76**, 094401 (2007).
[21]G. Li, P. Höpfner, J. Schäfer, C. Blumenstein, S. Meyer, A. Bostwick, E. Rotenberg, R. Claessen, and W. Hanke, Nat. Commun. **4**, 1620 (2013).
[22]Z. Q. Li, D. X. Zhang, and J. J. Lin, J. Appl. Phys. **99**, 124906 (2006).
[23]H. Wang, H. W. Zhao, T. Zhu, X. Li, and W. S. Zhan, J. Appl. Phys. **91**, 3111 (2002).
[24]H. Saito, S. Yuasa, and K. Ando, Phys. Rev. Lett. **95**, 086604 (2005).
[25]J. J. Robbins and C. A. Wolden, Appl. Phys. Lett. **83**, 3933 (2003).
[26]T. Yokobori, M. Okawa, K. Konishi, R. Takei, K. Katayama, S. Oozono, T. Shinmura, T. Okuda, H. Wadati, E. Sakai, K. Ono, H. Kumigashira, M. Oshima, T. Sugiyama, E. Ikenaga, N. Hamada, and T. Saitoh, Phys. Rev. B **87**, 195124 (2013).
[27]X. R. Li, M. J. Han, X. L. Zhang, C. Shan, Z. G. Hu, Z. Q. Zhu, and J. H. Chu, Phys. Rev. B **90**, 035308 (2014).
[28]T. Arnold, D. J. Payne, A. Bourlange, J. P. Hu, and R. G. Egdell, Phys. Rev. B **79**, 075102 (2009).
[29]M. Zenger, J. Moser, W. Wegscheider, D. Weiss, and T. Dietl, J. Appl. Phys. **96**, 2400 (2004).
[30]J. J. Krebs and G. H. Stauss, Phys. Rev. B **15**, 17 (1977).
[31]K. J. Jin, H. B. Lu, Q. L. Zhou, K. Zhao, B. L. Cheng, Z. H. Chen, Y. L. Zhou, and G. Z. Yang, Phys. Rev. B **71**, 184428 (2005).
[32]C. Mitra, P. Raychaudhuri, K. Dorr, K. H. Muller, L. Schultz, P. M. Oppeneer, and S. Wirth, Phys. Rev. Lett. **90**, 017202 (2003).